

Analytical Model of a Switched Reluctance Motor for its Optimization – Selected Problems

Abstract. An approach to modeling of a 6/4 type switched reluctance motor (SRM) is described in the paper. The modeling procedure is based on the reluctance network method and analytical solution of an ordinary differential equation. It allows for estimation of the torque, efficiency and acoustic noise of the motor taking into account the magnetic non-linearity and the control algorithm to keep a constant power. Some problems arising from the existence of mutual inductances are described as well. In a corresponding example eleven geometrical and winding parameters are supposed to be the input parameters in a corresponding synthesis program. Model is validated by means of FEM calculations. The proposed approach can be employed in designing and optimization of the SRM.

Streszczenie. W artykule zaprezentowano sposób modelowania silnika reluktancyjnego przełączalnego typu 6/4. Model oparty jest na metodzie sieci reluktancyjnych oraz quasi-analitycznym rozwiązaniu równania różniczkowego zwyczajnego i pozwala na wyznaczenie wielkości takich jak moment, sprawność, hałas magnetyczny, uwzględniając nieliniowość magnetyczną rdzenia i sposób sterowania na stałą moc, w oparciu o kilkanaście parametrów wejściowych charakteryzujących konstrukcję. Weryfikacja modelu została przeprowadzona metodą elementów skończonych. Proponowane podejście może być wykorzystane w projektowaniu i optymalizacji SRM. (Model analityczny silnika reluktancyjnego przełączalnego do wykorzystania w optymalizacji – wybrane problemy).

Keywords: switched reluctance motor, modeling, reluctance network, analytical calculations.

Słowa kluczowe: silnik reluktancyjny przełączalny, modelowanie, sieci reluktancyjne, obliczenia analityczne.

Introduction

A model of an electric motor, which could be used in its design and optimization process, should satisfy two usually contradictory requirements: high accuracy and high computational effectiveness. There are different strategies to reach this goal. A high accuracy can be achieved in models based on numerical field calculations, for example FEM models, but a disadvantage is their relatively low effectiveness. Much higher effectiveness can be achieved in models based on simple analytical calculations. Unfortunately, an important constraint of the analytical models is their relatively low accuracy. For this reason analytical models are usually verified by means of experiments and/or corresponding FEM models.

A model used in electric motor design process should be able to estimate quantities representing motor properties. More important are: load current, electromagnetic torque, speed, efficiency and motor cost under some assumed operation conditions (supplying voltage, temperature, and load). Sometimes, for instance in SRM, additional parameters like acoustic noise or torque ripples are very important.

Many papers devoted to optimization of the SRM are based on FEM models with auxiliary lumped parameter parts defined by means of analytical formulae [1], [2], [3]. The lumped parameter model proposed in this paper is based only on analytical calculations, which concern magnetic circuit (reluctance network method) and transient simulations (quasi-analytical solution of an ordinary differential equation). Arising nonlinear algebraic equations are solved numerically. The presented model is a summary of a research work started by the authors a few years ago [4]-[6].

A base initial construction in modeling is a 6/4 type SRM described in [7]. According to experimental results used in model validation there, it can be considered as a credible relevance in a verification process performed for other models. The following motor parameters were considered to be of prime interest for the analyzed SRM: the mean value of the electromagnetic torque, the relation of the mean to max value of the electromagnetic torque, efficiency, magnetic noise level and motor mass. Model enables determining all quantities necessary to define criterial functions and feasible region in optimization, in particular

the power loss components, the electromagnetic torque parameters, the magnetic radial force, for a constant angular velocity. It takes into account the magnetic non-linearity based on a M400-50A electrical sheet with specific loss 3.74 W/kg (for 1.5T/50Hz). Mutual inductances are neglected in the model, but consequences of this assumption are discussed. The proposed model is a main part of a synthesis program in motor construction optimization.

Validation of the proposed SRM analytical model has been performed by means of 2D FEM analysis, but some results were referred to an experimental data given in [7] and [8] as well.

Analytical model and synthesis program of the SRM

Description of the Model

The model enables determining all important motor quantities, for instance the load phase current, electromagnetic torque, flux density in the stator pole, and radial force acting on stator pole of the SRM, as time functions dependent on motor parameters and operation conditions, with accuracy required for gradient optimization routines. A constant velocity and one pulse mode operation of the motor is assumed in the computation. Some preliminary results had been published in [5], other detailed information can be found in [6].

The set of input quantities in the synthesis program comprises such motor parameters as: geometrical dimensions $r_o, r_{sy}, r_{sp}, r_{ry}, r_{shs}, b_{sp}, b_{rp}, g$ (Fig. 1), core length l , the number of turns per phase winding N_{iph} , diameter of a conductor, the DC voltage E supplying phase circuit, the rotor angular velocity $\omega = n \cdot \pi / 30$ and assumed input active power P_{in} .

At the beginning of calculations based on the reluctance network method, the phase winding inductance $L(i, \varphi)$ is determined as a function of phase current i and angular rotor position φ . In this approach the cross-section area of the core is divided on a number of regions with constant magnetic flux called "flux tubes", see Fig. 2. Some numerical experiments had been performed to check an influence of tubes number and their arrangement on calculation accuracy (basing upon FEM calculations related to the initial construction) and time. It had been found that 6

tubes offer the best compromise for the analyzed construction. Solving non-linear algebraic equations describing elementary magnetic circuits for all tubes makes it possible to calculate necessary quantities, in particular the phase winding inductance $L(i, \varphi)$.

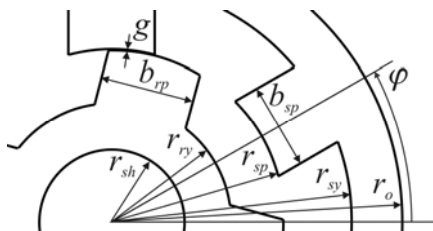


Fig.1. Geometrical parameters of the construction

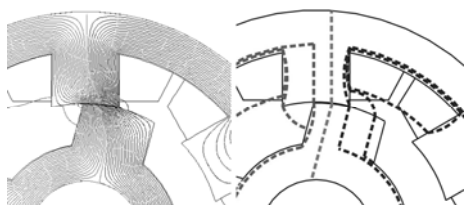


Fig.2. Magnetic field in the SRM core and a corresponding flux tubes arrangement for a selected rotor position $\varphi = 75^\circ$

This function must be smooth enough to protect gradient optimization routines from a prematurely stop and wrong calculation results. The following approach has been applied in the model to achieve this goal. Firstly, a set of predefined rotor positions $\{\varphi_a, \varphi_b, \varphi_c, \varphi_d, \varphi_e\}$ selected partly after [9] and [10], starting from unaligned rotor position $\varphi_a = 0$ and ending at the aligned one $\varphi_e = \pi N_r$ (where N_r is a number of rotor poles), together with additional sets of equispaced positions in each subinterval, have been defined, see Appendix A.

Next, a smoothing spline function has been applied to the set of inductance values $\{L(\varphi_a), \dots, L(\varphi_e)\}$. A periodicity property of the $L(\varphi)$ is sufficient to extend this function to any desired interval of the rotor position φ .

In the next step, basing upon the $L(\varphi)$, a function of a flux linkage $\Psi(i, \varphi)$ and its both partial derivatives are calculated.

The phase winding resistance R results from dimensions of the stator pole and winding parameters. In the paper it comprises an additional resistance representing internal resistance of the constant voltage source, the supplying wires, and the converter elements as well.

The torque function T_{el} in the model results from a magnetic co-energy function differentiation:

$$(1) \quad T_{el}(i_x, \varphi) = \frac{\partial}{\partial \varphi} \int_0^{i_x} L(i, \varphi) di$$

The phase current function $i(t)$ is determined as an quasi-analytical (piece-wise constant) solution of the following non-linear differential equation:

$$(2) \quad u = Ri + \frac{\partial \Psi(i, \varphi)}{\partial i} \frac{di}{dt} + \omega \frac{\partial \Psi(i, \varphi)}{\partial \varphi}$$

where: u – phase voltage, i – phase current, t – time, ω – angular velocity, φ – angular rotor position, Ψ – flux linkage,

R – phase resistance.

The equation (2) is solved in the paper for a constant angular velocity $\omega = n \cdot \pi / 30$, for $n = 3500$ rpm, and a phase voltage function $u(t)$ defined below:

$$u(0) = E; \quad i(0) = 0; \quad i \geq 0$$

$$(3) \quad u = \begin{cases} E, & \text{if } 0 \leq \varphi \leq \varphi_{off} \text{ and } i \geq 0 \\ -E, & \text{if } \frac{2\pi}{N_r} \geq \varphi > \varphi_{off} \text{ and } i > 0 \\ 0, & \text{if } \frac{2\pi}{N_r} \geq \varphi > \varphi_{off} \text{ and } i = 0 \end{cases}$$

The equation (2) is solved only for one phase. The voltage E is assumed in the paper to be 160 V (or 215 V for higher rotor speeds $n > 5000$ rpm). The assumption $i \geq 0$ in (3) results from an assumed inverter configuration. The φ_{off} angle is a solution of a proper non-linear algebraic equation in each optimization iteration, to obtain the required reference value of the motor input active power $P_{in} = 35$ kW. This input power is used as a reference instead of output one, what is a common case, because this way the calculation procedure in the model became much simpler at a little loss of accuracy. Both poles of one phase are connected in parallel. The above assumptions concern all calculations performed in this paper.

Troubles with a convergence of the optimization routine appear when the equation (2) is solved numerically [4]. Fortunately, the partial derivatives of the flux linkage can be represented by its piece-wise constant approximation to solve (2) analytically with a good accuracy. These partial derivatives are calculated for all subsequent time intervals $[t_0^k, t_e^k]$, where $t_0^{k+1} = t_e^k$, $k = 0, 1, 2, \dots$, using look-up tables, see Appendix B.

The input power value $P_{in} = 35$ kW was selected to be approximately the same power value as that achieved in [7] by the real machine for the rotor velocity $n = 3500$ rpm.

In the next step the following quantities are calculated: the maximal values of the flux density in main motor parts (denoted by the subscripts $x = rp, ry, sp, sy$, see Fig. 3), time functions of a torque, and a magnetic radial force.

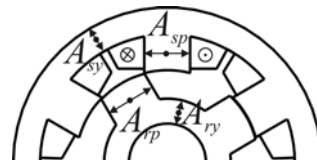


Fig.3. A scheme for flux density calculations

The flux density B_{mx} in a motor part “ x ” has been calculated according to the formula:

$$(4) \quad B_{mx} = \max_{t \in \left[0, \frac{1}{4} \frac{\omega}{2\pi}\right]} \left(\frac{k_{\phi x} \cdot \phi(t)}{A_x} \right)$$

where $k_{\phi x} = 1$ for poles and $k_{\phi x} = 0,5$ for yokes, $\phi(t)$ is a magnetic flux time function, and the quantity A_x is a cross-section area of a corresponding motor part (Fig. 3).

The magnetic radial force F_{rad} is calculated from the formula:

$$(5) \quad F_{rad}(i, \varphi) = L_{4Frads}(i, \varphi) \cdot \left| \frac{\left(\phi_{aligned} \left(i, \varphi = \frac{\pi}{4} \right) \right)^2}{2\mu_0 l \left(\frac{r_{sp} - g}{2} \beta_s + \beta_r + g \right)} \right|$$

where $L_{4Frad}(i, \varphi)$ is an auxiliary inductance function, which takes the advantage of the similarity of shapes of functions $L(i=\text{const}, \varphi)$ and $F_{rad}(i=\text{const}, \varphi)$ (see Fig. 4 and Fig. 5):

$$(6) \quad L_{4Frad}(i = i^*, \varphi) = \frac{L(i = i^*, \varphi) - \min(L(i = i^*, \varphi))}{\max(L(i = i^*, \varphi)) - \min(L(i = i^*, \varphi))}$$

The other quantities in (5) are: β_s, β_r – the stator and rotor pole arcs, g – the air-gap length (Fig. 1), l – the stack length, r_{sp} – the stator pole radius (Fig. 1), μ_0 – the magnetic permeability of a vacuum, and $\phi_{aligned}$ – the magnetic flux at an aligned position of the rotor.

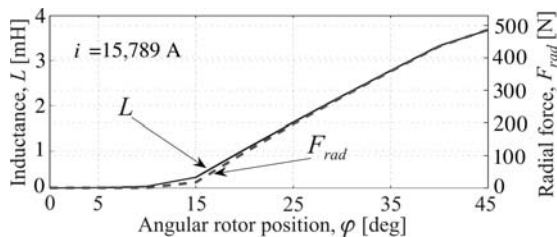


Fig. 4. Inductance function L and a magnetic radial force F_{rad} versus angular rotor position for a constant, low current value (no saturation, FEM calculations results)

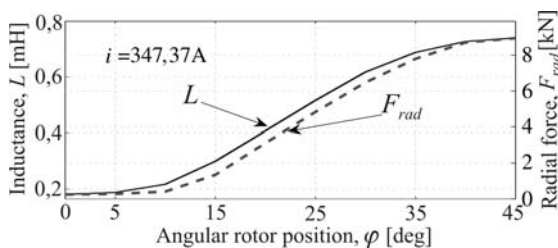


Fig. 5. Inductance function L and a magnetic radial force F_{rad} versus angular rotor position for a constant, high current value (saturation, FEM calculations results)

Output parameters of the model – quantities for motor optimization

All important quantities, which can be used in the synthesis program to define criterial functions and a feasible region are derived in the model: the average value T_{av} of electrical torque function $T_{el}(t)$, the ratio of the T_{av} to the max T_{el} (the torque ripples quantity T_{av2max}), efficiency η , acoustic noise level L_{wd} (a magnetic component) and total mass m_m (or the cost of materials).

If the function $T_{el}(t)$ is an electromagnetic torque produced by one phase current, then:

$$(7) \quad T_{av} = N_{ph} N_r \frac{\omega}{2\pi} \int_0^{\frac{1}{N_r} 2\pi} T_{el}(t) dt$$

and:

$$(8) \quad T_{av2max} = \frac{T_{av}}{\max(T_{el}(t))}$$

The above relationships are correct if the current values in two phases during the commutation do not cause the saturation (it is possible in the analysed cases if holds $0^\circ \leq \varphi_{off} \leq 30^\circ$). This assumption reduces calculation time and improves the optimization calculation convergence.

If V_j is a volume of a j th motor element characterized by its specific mass ρ_j , than the material mass m_m of the motor is:

$$(9) \quad m_m = \sum_j V_j \rho_j$$

The motor efficiency is defined in the paper as:

$$(10) \quad \eta = \frac{P_{in} - \Delta P_{Fe} - \Delta P_{Cu} - \Delta P_{mech}}{P_{in}} \cdot 100\%$$

where active power components are:

- P_{in} – input active power

$$(11) \quad P_{in} = \frac{\omega}{2\pi} N_r N_{ph} \int_0^{\frac{1}{N_r} 2\pi} u i dt \cong \frac{\omega}{2\pi} N_r N_{ph} \sum_k \int_{t_0^k}^{t_e^k} u^k i^k dt$$

The procedure of integration calculations has been reduced to one stator phase winding and a revolution angle equal to one rotor pole pitch. The integration is performed in each k th time interval $[t_0^k, t_e^k]$, see the description of solving procedure of the equation (2) in Appendix B.

- ΔP_{Cu} – electrical loss in the stator winding

$$(12) \quad \Delta P_{Cu} = \frac{\omega}{2\pi} N_r N_{ph} \frac{R_{pole}}{2} \int_0^{\frac{1}{N_r} 2\pi} i^2 dt$$

R_{pole} is a resistance of one pole winding.

- ΔP_{Fe} – iron loss in the magnetic core

$$(13) \quad \Delta P_{Fe} = \sum_x (\Delta P_{Fehx} + \Delta P_{Feex})$$

where ΔP_{Fehx} and ΔP_{Feex} are hysteresis and eddy-current loss components in the “x” core part, see Fig. 3.

An accurate determining of the iron loss is difficult due to a complex shape of the flux density functions in different core parts [11]. In the paper the iron losses are estimated in a simplified way, basing upon an assumption that the functions of magnetic flux density in motor core parts can be approximated by means of a linear spline. The example of the flux density function on Fig. 6 justifies this decision.

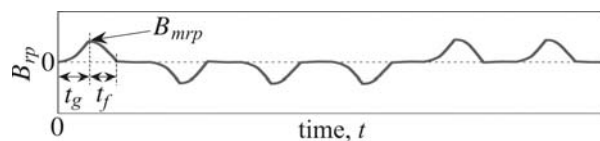


Fig. 6. Flux density function B_{mp} in the middle of the rotor pole for one complete rotation of the rotor (FEM calculations for $n = 3500$ rpm)

If the flux density function in the rotor pole is as on Fig. 6, then:

$$(14) \quad \Delta P_{Fehrp} = C_h ((N_s - 4) \cdot 0.4 + 2) \frac{\omega}{2\pi} B_{mp}^2 N_r V_{rp} k_{stk}$$

and:

$$(15) \quad \Delta P_{Feerp} = C_e \left[\left(\frac{B_{mp}}{t_g} \right)^2 t_g + \left(\frac{B_{mp}}{t_f} \right)^2 t_f \right] \cdot N_s \frac{\omega}{2\pi} N_r V_{rp} k_{stk}$$

where V_{rp} is the rotor pole volume, C_h and C_e are the coefficients of hysteresis and eddy-current losses, k_{stk} is the stacking factor, N_s is a number of stator poles. The total iron loss value can be obtained after applying a similar procedure to the other parts of the magnetic core, basing upon corresponding flux density functions presented on Figures 5 and 6 in [4]. The constant 0.4 in (14) represents minor hysteresis loops according to [11]. The above procedure worked out for calculation of iron losses can be employed if $\varphi_{off} \leq 30^\circ$.

- ΔP_{mech} – mechanical power loss [2]

$$(16) \quad \Delta P_{mech} = 1.3(1 - 2r_o)(0.1 \cdot n)^2 (2r_o)^4$$

where n [rpm] is the rotor speed.

Acoustic Noise

In the paper the acoustic noise prediction is based on a simplified analytical model described in [12], [13], [14]. It comprises the following analyzed components: determining a magnetic radial force time function, a frequency domain analysis of the radial force, a modal analysis of the stator, determining amplitude of dynamic deflection of the stator, and a sound power radiated by the motor.

The magnetic radial force time function in the SRM is a non-sinusoidal waveform and the acoustic noise analysis must be performed for every important sinusoidal component of the radial force time function. Moreover, the sound power level of every frequency component should be weighted (using A-weighting curve) because of the human ear properties. The A-weighted sound power levels L_{wAh} for every h th order frequency component are combined to give one single value L_{wA} , which enables an effective comparison of different constructions of the motor:

$$(17) \quad L_{wA} = 10 \log \left(\sum_h 10^{0.1L_{wAh}} \right)$$

The noise level is analysed on the area of the source of radiation. The sound power level L_w related to a frequency component f_{exc} can be expressed as:

$$(18) \quad L_w(f_{exc}) = 10 \log \left(\frac{P_{sound}(f_{exc})}{P_{sound,ref}} \right)$$

where $P_{sound,ref}$ is a reference sound power equal to 10^{-12} W, and P_{sound} is the sound power radiated by the motor:

$$(19) \quad P_{sound}(f_{exc}) = \sum_m 4\sigma_{rel} \rho_{air} c_{air} \pi^3 f_{exc}^2 D_{circum}^2 r_o l$$

where: f_{exc} – excitation frequency, σ_{rel} – modal radiation efficiency [13], c_{air} – travelling speed of sound in the air (m/s), ρ_{air} – density of air (kg/m^3), m – order of a mode (-) D_{circum} – amplitude of dynamic deflection [12], [13].

The modes $m = 0, 2, 4$ representing the majority of sound power for 6/4 type SRM [14] are considered in the model.

Model Validation

The quality of the optimization results depends strongly on an accuracy of the applied model. The validation calculations concerning the analytical model used in the paper have been performed in two ways. Firstly – by means of a 2D finite element analysis, and secondly – by means of a comparison with experiments described by other authors for the same switched reluctance machine [7], [8].

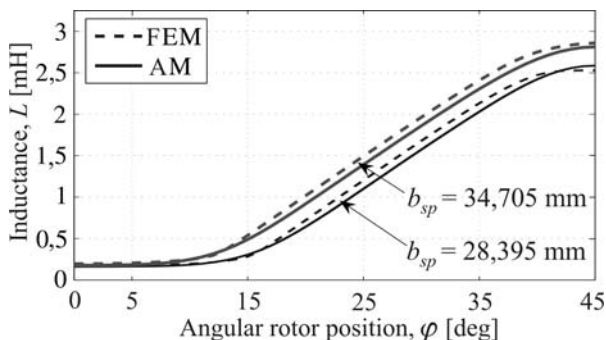


Fig. 7. A comparison of phase inductance function $L(\varphi)$ obtained by analytical model (AM) and finite element model (FEM), for two values of the b_{sp}

Firstly the comparison has been performed for the phase inductance function $L(\varphi)$ calculated for different values of geometrical parameters (and constant current).

Calculation results for two values of the b_{sp} : 10% higher and 10% lower in relation to the base construction from [7] are shown on Fig. 7.

Some verification results for the E-M torque of the base construction are shown on Fig. 8, as a comparison of static torque functions for a few constant values of the current.

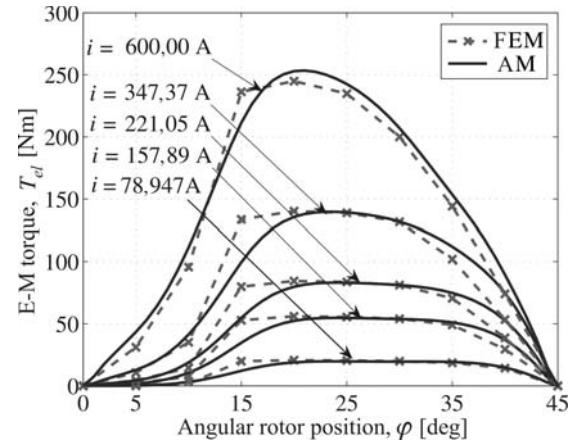


Fig. 8. A comparison of static torque function obtained by analytical model (AM) and finite element model (FEM), for a few constant values of the phase current (base construction)

Secondly, the comparison had been done for time domain simulations at constant rotor speed, under conditions described in the second paragraph, but for an arbitrarily imposed turn-off angle φ_{off} . The phase current functions obtained for both the analytical and FEM models are shown on Fig. 9.

An important assumption in the paper is that the influence of mutual inductances can be neglected. Two tests of motor operation with the help of FEM analysis have been performed to check its validity. In the first one only one phase was supplied (like in the analytical model, without the mutual inductances; it is denoted "1 phase supplied" on Fig. 9), and in the second one - all three phases were supplied, (the "3 phases supplied" case on Fig. 9) according to control algorithm. In experiments, if a phase is switched on at $\varphi = 0^\circ$, the next one is supplied at $\varphi = 360/N_{ph}/N_r$, where N_{ph} is the number of stator phases (it is a characteristic value for the analysed motor, $\varphi = 30^\circ$).

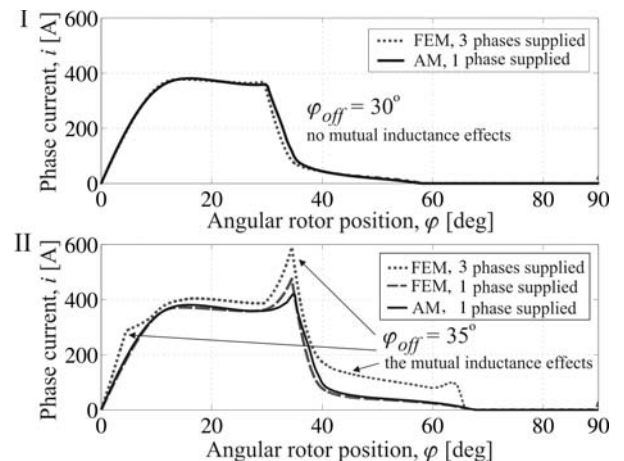


Fig. 9. Influence of mutual inductances. A comparison of phase current functions obtained by analytical (AM) and finite element models (FEM), for two values of the φ_{off} , and two cases of FEM simulations – for all three phases supplied, and for one phase

Usually a value of a mutual inductance is small in comparison to a value of the main inductance.

Unfortunately, if saturation occurs, the both inductance values can be of the same order. To examine it, the “1 phase supplied” case of the analytical model and “3 phases supplied” case of the FEM model have been performed twice: firstly – when the first phase is switched off at $\varphi = 30$ degrees (Fig. 9.I), and secondly – when the first phase is switched off at $\varphi = 35$ degrees (Fig. 9.II). In the second case the influence of the mutual inductance is remarkable - when the first phase is switched off at $\varphi = 35$ degrees, instead of 30 degrees, the current in the next phase is already about 200 A and the saturation occurs.

Fig. 10 shows a comparison of time domain torque function at constant speed 3500 rpm, for three different values of the b_{sp} .

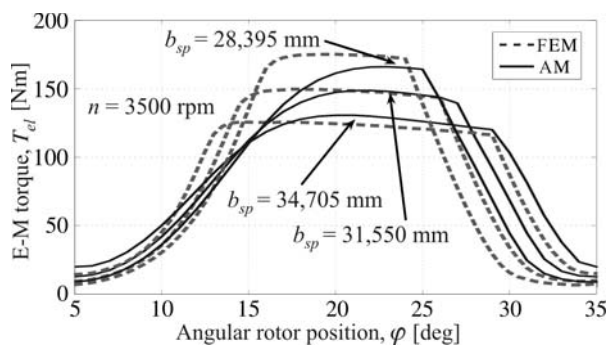


Fig. 10. A comparison of time domain torque function obtained by analytical model (AM) and finite element model (FEM), for different values of the b_{sp} , at constant speed

Table 1. Output parameters of the analytical model in comparison to the FEM model, for three different values of the b_{sp}

Output parameter	b_{sp} , [mm]				
	31,550	34,705		28,395	
	Base value	New value	Relative change (%)	New value	Relative change (%)
$P_{in,AM}$ [kW]	35,00	35,00	0,00	35,00	0,00
$P_{in,FEM}$ [kW]	35,24	35,17	-0,20	35,44	0,58
$\varphi_{off,AM}$ [°]	26,94	29,28	8,71	25,22	-6,37
$\varphi_{off,FEM}$ [°]	26,29	29,16	10,91	24,06	-8,49
$T_{av,AM}$ [Nm]	88,20	89,87	1,89	86,22	-2,25
$T_{av,FEM}$ [Nm]	86,94	87,83	1,02	85,87	-1,24
$T_{av2max,AM}$ [-]	0,59	0,68	15,48	0,52	-12,48
$T_{av2max,FEM}$ [-]	0,57	0,69	21,11	0,48	-15,69
$F_{radmax,AM}$ [kN]	7,06	7,69	8,91	6,51	-7,89
$F_{radmax,FEM}$ [kN]	5,23	6,41	22,43	4,36	-16,73
$F_{radav,AM}$ [kN]	1,41	1,71	21,46	1,19	-15,46
$F_{radav,FEM}$ [kN]	1,05	1,44	36,99	0,82	-22,02
$L_{wA,AM}$ [dB]	97,48	95,39	-2,15	95,56	-1,97
$L_{wA,FEM}$ [dB]	91,83	93,31	1,62	90,45	-1,50
$\Delta P_{Fe,AM}$ [kW]	0,63	0,68	7,89	0,61	-3,17
$\Delta P_{Fe,FEM}$ [kW]	0,63	0,71	11,75	0,59	-7,41
$\Delta P_{Cu,AM}$ [kW]	1,47	1,27	-13,41	1,70	15,55
$\Delta P_{Cu,FEM}$ [kW]	1,40	1,17	-16,31	1,68	19,93
η_{AM} [%]	93,27	93,69	0,45	92,68	-0,64
η_{FEM} [%]	93,50	93,93	0,46	92,88	-0,66

AM – Analytical Model, FEM – Finite Element Method

(*) calculated in the same way as in the analytical model, but for radial force obtained from finite element model.

A comparison of the proposed FEM model with the results of measurements presented in the papers [7] and [8] has been shown on Fig.11. There is a level of uncertainty of the results on Fig.7 caused by the assumptions in the proposed model, in particular:

- no PWM, only one-pulse mode supplying voltage,
- a constant turn-on angle $\varphi_{on} = 0^\circ$,
- the converter consists of ideal elements.

Very likely electrical steel properties in the models are not the same as in [7].

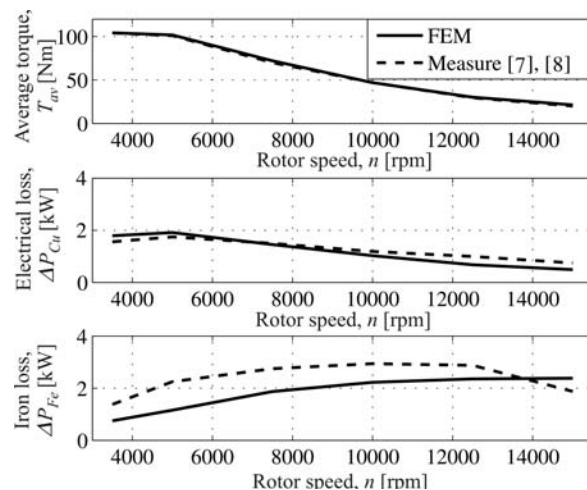


Fig. 11. The comparison of some quantities for the proposed FEM model and the real machine [7], [8]

Output parameters obtained with the help of both the analytical and finite element models are presented in Table 1.

Conclusions

The computer program used in the paper was implemented in Matlab environment. The time of calculations performed for one call of the synthesis program (determining all criterial and constraint functions) was below 60 sec on a PC with Intel PIV 3.0GHz processor. The proposed approach seems to be useful when searching for the best design of an SRM. It can be expected that an extension of the model by a better representation of an inverter, considering the mutual inductances of the stator phase winding as well as heating model, would increase the credibility of optimization results.

Due to verification results in Table 1 for the magnetic noise level it seems to be justified searching for some other criterial function, representative for the noise, to be used in optimization [5], [6].

The described modeling procedure allows applying gradient routines in optimization process and increasing its effectiveness.

Appendix A : Rotor positions used in calculations

$$\left. \begin{aligned}
 \varphi_a &= 0 \\
 \varphi_b &= \begin{cases} \frac{\pi}{N_r} - \frac{\beta_s}{2} - \arcsin\left(\frac{b_{rp}}{2 \cdot r_{ry}}\right) \dots \\ \dots \text{ for } \frac{\beta_s}{2} + \arcsin\left(\frac{b_{rp}}{2 \cdot r_{ry}}\right) < \frac{\pi}{N_r} \\ 0 \text{ for } \frac{\beta_s}{2} + \arcsin\left(\frac{b_{rp}}{2 \cdot r_{ry}}\right) \geq \frac{\pi}{N_r} \end{cases} \\
 \varphi_c &= \begin{cases} \frac{\pi}{N_r} - \frac{\beta_s}{2} - \frac{\beta_r}{2} \text{ for } \frac{\beta_s}{2} + \frac{\beta_r}{2} < \frac{\pi}{N_r} \\ 0 \text{ for } \frac{\beta_s}{2} + \frac{\beta_r}{2} \geq \frac{\pi}{N_r} \end{cases} \\
 \varphi_d &= \begin{cases} \frac{\pi}{N_r} + \frac{\beta_s}{2} - \frac{\beta_r}{2} \text{ for } \beta_s \leq \beta_r \\ \frac{\pi}{N_r} - \frac{\beta_s}{2} + \frac{\beta_r}{2} \text{ for } \beta_s > \beta_r \end{cases} \\
 \varphi_e &= \pi/N_r
 \end{aligned} \right\} (1.A)$$

where $\beta_s = 2^* \sin^{-1}(b_{rp}/(2^* r_{sp}))$, $\beta_r = 2^* \sin^{-1}(b_{rp}/(2^*(r_{rs} - g)))$

are the stator and rotor pole arcs angles.

APPENDIX B. AN APPROXIMATE ANALYTICAL SOLUTION OF EQUATION (2) CAN BE DERIVED AS FOLLOWS.

If in an k 'th time interval $[t_0^k, t_e^k]$, ($t_0^{k+1} = t_e^k$, $k = 0, 1, 2, \dots$), we can assume that:

$$\left. \begin{aligned} \frac{\partial \Psi(i, \varphi)}{\partial i} \Big|_{t \in [t_0^k, t_e^k]} &\cong \frac{\partial \Psi(i, \varphi)}{\partial i} \Big|_{t = t_0^k} = C_i^k \\ \frac{\partial \Psi(i, \varphi)}{\partial \varphi} \Big|_{t \in [t_0^k, t_e^k]} &\cong \frac{\partial \Psi(i, \varphi)}{\partial \varphi} \Big|_{t = t_0^k} = C_\varphi^k \end{aligned} \right\} (1.B)$$

than an analytical solution of the equation (2) in the k th interval exists and can be presented in the form:

$$i^k(t) = \begin{cases} \frac{\exp\left(\frac{-R(t - C^k)}{C_i^k}\right) - u^k + \omega C_\varphi^k}{-R}, & \text{if } u^k - \omega C_\varphi^k - R i_0^k > 0 \\ \frac{\exp\left(\frac{-R(t - C^k)}{C_i^k}\right) + u^k - \omega C_\varphi^k}{-R}, & \text{if } u^k - \omega C_\varphi^k - R i_0^k < 0 \\ \frac{R}{-u^k + \omega C_\varphi^k}, & \text{if } u^k - \omega C_\varphi^k - R i_0^k = 0 \end{cases} (2.B)$$

where $t \in [t_0^k, t_e^k]$; u^k , ω and R (see par. *Description of the Model*) are constant for a k ; $i_0^k = i^{k-1}(t_e^{k-1})$; C^k is a constant, which results from initial conditions:

$$C^k = t_0^k + \frac{1}{R} C_i^k \ln |u^k - \omega C_\varphi^k - R i_0^k| (3.B)$$

REFERENCES

- [1] K. M. Rahman, and S. E. Schulz, "Design of High-Efficiency and High-Torque-Density Switched Reluctance Motor for Vehicle Propulsion," *IEEE Transactions on Industry Applications*, Vol. 38, No. 6, 2002, pp. 1500-1507.
- [2] A. Matveev, "Development of Methods, Algorithms and Software for Optimal Design of Switched Reluctance Drives," Ph.D. dissertation, Eindhoven Univ. of Techn., Eindhoven, 2006.
- [3] M. N. Anwar, I. Husain and A. V. Radun, "A Comprehensive Design Methodology for Switched Reluctance Machines,"

IEEE Transactions on Industry Applications, Vol. 37, No. 6, 2001, pp. 1684-1692.

- [4] W. Jazdzynski, and M. Majchrowicz, "An Approach to Find an optimum Designed SRM for electric vehicle drive", *Proceedings of the 2008 International Conference on Electrical Machines*, Paper ID 1391, 6-9 September 2008, Vilamoura, Portugal.
- [5] M. Majchrowicz, and W. Jazdzynski, "Selected Problems of Optimization of a Switched Reluctance Motor for an Electric Vehicle using Analytical Calculations", *International Conference on Renewable Energies and Power Quality (ICREPQ'10)*, Paper ID 483, 23-25 March 2010, Granada, Spain.
- [6] M. Majchrowicz, "Optimization of the Switched Reluctance Motor for an Electric Vehicle Drive," Ph.D. thesis (in Polish), AGH University of Science and Technology, Krakow, 2011, unpublished.
- [7] H. Bausch, A. Greif, B. Lange, and R. Bautz, "A 50kW/15000rpm Switched Reluctance Drive for an Electric Vehicle: Current Control and Performance Characteristics," *Proceedings of XIV International Conference on Electrical Machines*, pp. 603-607, 28-30 August 2000, Espoo, Finland.
- [8] H. Bausch, A. Greif, A. B. A. Nickel, "A Switched Reluctance and an Induction Machine in a Drivetrain for an Electrical Vehicle Under the Conditions of a Car Application" *Proceedings of XIV International Conference on Electrical Machines*, pp. 1313-1316, 28-30 August 2000, Espoo, Finland.
- [9] R. Krishnan, *Switched Reluctance Motor Drives: Modeling, Simulation, Analysis, Design, and Applications*, CRC Press LLC, Boca Raton, 2001.
- [10] P. Vijayraghavan, "Design of Switched Reluctance Motors and Development of a Universal Controller for Switched Reluctance and Permanent Magnet Brushless DC Motor Drives," Ph.D. thesis, Virginia Polytechnic Institute and State University. of Techn., Blacksburg, 2001.
- [11] Y. Hayashi, and T. J. E. Miller, "A New Approach to Calculating Core Losses in the SRM," *IEEE Transactions on Industry Applications*, Vol. 31, No. 5, 1995, pp. 1039-1046.
- [12] M. N. Anwar, and I. Husain, *Radial Force Calculation and Acoustic Noise Prediction in Switched Reluctance Machines*, IEEE Trans. on Industry Applications, Vol. 36, No. 6, 2000, pp. 1589-1597.
- [13] J. F. Gieras, C. Wang, and J. C. Lai, *Noise of Polyphase Electric Motors*, CRC Press, Taylor & Francis Group, Boca Raton, 2006.
- [14] P. O. Rasmussen, F. Blaabjerg, J. K. Pedersen, P. C. Kjaer, and T. J. E. Miller, "Acoustic noise simulation for Switched Reluctance Motors with audible output", *Proceedings of European Conference on Power Electronics and Applications*, 1999, Lausanne, Switzerland.

Authors: dr hab. inż. Wiesław Jazdzynski, prof.nz.AGH, AGH University of Science and Technology, Al. Mickiewicza 30, 30-059 Kraków, E-mail: wjaz@agh.edu.pl, dr inż. Michał Majchrowicz, Nidec Motors & Actuators (Poland), Sp. z o.o., ul. Skarbowa 36, 32-005 Niepolomice, E-mail: michal.majchrowicz@nidec-ma.com